Shapes and Self-Movement in Protocell Systems

Keisuke Suzuki*,**
The University of Tokyo

Takashi Ikegami**
The University of Tokyo

Abstract The effect of shapes on self-movement has been studied with an extended model of autopoiesis. Autopoiesis is known as a theory of self-boundary maintenance. In this study, not only the autopoietic generation of the self-boundary, but also the emergence of self-motility, has been examined. As a result of computer simulations, it has been found that different membrane shapes cause different types of self-movement. A kind of chemotaxis has been observed for some shapes. The mechanism of chemotaxis is discussed by studying the internal chemical processes within the shape boundaries.

Keywords
Autopoiesis, chemotaxis, sensory-motor coupling, shapes, self-boundary

1 Introduction

Self-movement is a fundamental feature that distinguishes life from nonlife forms. It is not simply an outcome of the internal dynamics of a cell, but is a result of recurrent couplings between an environment and internal dynamics. These couplings can be characterized as an *interface*, which filters and amplifies the inward and outward flow of chemicals across the cell boundary. The interface is realized by a biological membrane that must be self-generated by a cell's chemical reaction. More importantly, the interface isn't a plain unstructured sheet, but can be a folded geometrical object. We try to capture this geometrical nature of the interface and propose a protocell model, which shows self-movement driven by the membrane shapes. We then raise the following question: When does a chemical network bounded by a membrane become a *cell* that has its own intention? In the other words, we try to make a consistent connection between local chemical processes driven by noise and the global sensory-motor coupling of a cell. Our conjecture is that the geometrical shape of a membrane can mediate sensor and motor activities of a cell.

Regarding real cell systems, we know that many biological cells show self-motility, for example, *Amoeba proteus*, one of a class of protozoa that exhibits dynamic motility patterns in response to environmental changes. They move around the environment and forage by drastically changing their shape patterns [23]. We name those dynamic processes *amoebic movement*. The movement is principally generated by chemical machinery consisting of actin and myosin proteins across the entire cell structure. More sophisticated modern cells use a special organ called a flagellum [22, 21, 16]. The mechanism of the cell motion is well studied by simulating the physico-chemical processes of actin dynamics [8, 2]. Such cells self-move by responding to environmental differences, such as chemical gradients. Given attractant chemicals, cells sense the attractant and aggregate to it, a process often called *chemotaxis*. A cell may sense the attractant gradient by making use of internal chemicals [13, 17]. There have been some simulation studies that qualitatively reproduced amoebic cell motions as well as chemotaxis [1, 12].

* Contact author.
** Department of General Systems Sciences, The Graduate School of Arts and Sciences, The University of Tokyo, 3-8-1 Komaba, Tokyo, 153-8902, Japan. E-mail: ksk@sacral.c.u-tokyo.ac.jp

In comparison with those studies, we incorporate the membrane shape more explicitly into our model, which is an extension of the simple cell model proposed by Varela et al. [19] and later by McMullin and Varela [10]. The cell model consists of particles reproducing a membrane, which then restricts the region in which a chemical reaction occurs. Due to the localization of the chemical reaction in the region, the membrane is regenerated. This cyclic structure forms an entity that we call a *cell*. We extend the model by introducing explicit membrane dynamics. Each membrane particle moves randomly, but at the same time it is highly constrained by the neighboring connected particles. Now the question becomes more explicit: how such a locally fluctuating membrane configuration can support global coherent cell motion.

It should be reminded that our purpose is not suppressing any fluctuation at the micro level to get robust coherence at the macro level. For example, with respect to chemotaxis, we pay attention to the associated motion fluctuation. What we call biological autonomy is the autonomous dynamics of a living system that shows different behaviors in the same conditions, or the same behaviors in different conditions. In this article, we will simulate chemotaxis accompanying behavior fluctuation introduced by the membrane shapes.

In Section 2, we describe the model. In Section 3, cell movement and chemotactic behavior in certain conditions are reported. In Section 4, we analyze the spatial fluctuation of the membrane configuration. In Section 5, we discuss how a certain membrane shape can substitute for sensors.

2 The Model

The notion of autopoiesis was proposed by Varela et al. as a method to find the logic of a life form as a self-maintaining entity [19, 18]. Varela clarified the concept by building an abstract chemical system that has a metabolic cycle among substrates (SUBSTRATE), catalysts (CATALYST), and link (LINK) particles. The model is often called the substrate-catalyst-link (SCL) model [10]. These particles move around randomly in a two-dimensional discrete space.

Surrounding a CATALYST, LINK particles form a membrane, which is maintained recurrently and dynamically. An autopoietic cell is characterized by this self-cyclic nature of metabolism. We have modified this basic algorithm to include a variety of membrane shapes. Instead of having the decay process of the LINK particles, we have designed new rules for replacing the LINK particles without breaking the membrane. This modification causes the membrane size to vary from a minimum length of four units to infinity. The following subsections give the details of the modified SCL model.

2.1 Basic Settings

Three types of abstract particles are defined in the model. There is only one unique CATALYST (C) particle that exists in the space. The CATALYST particle cannot occupy the same site as other particles. The LINK (L) particle has two different forms: free-running or chain-linked (where particles are bonded to one another). The forms of the LINK and the SUBSTRATE (S) are not mutually exclusive. Each particle, except the bonded LINK particle, moves randomly with certain probabilities when there is space around it.

A cell configuration is defined as a set of bonding LINK particles that enclose one CATALYST particle. The SUBSTRATE particles can be anywhere in the environment or in the cell. The CATALYST particles never pass through the membrane, but the SUBSTRATE particles do. So, the metabolic process occurs only within the membrane. A diagram of a cell structure is shown in Figure 1.

2.2 A Metabolic Cycle

The chemical reaction used in our model has been inherited from the original model. The CATALYST particle creates a free LINK particle when two SUBSTRATE particles are in the neighborhood of the CATALYST:

$$S + S + C \rightarrow L + C \quad (1)$$

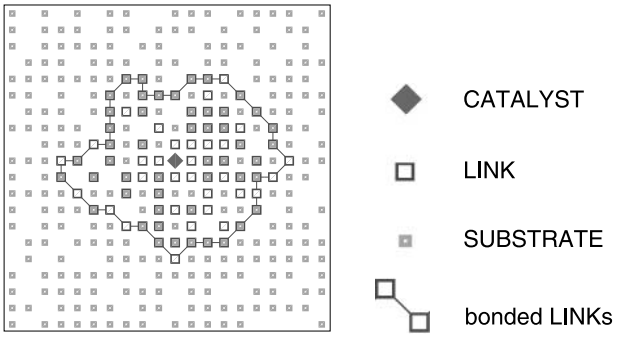

Figure 1. An example of a membrane shape in the two-dimensional plane.

The new free LINK particles diffuse in the cell and will be inserted into the membrane loop. The insertion of the free LINK particles into the bonded LINK particles occurs when the LINK particles enter the neighborhood of obliquely bonded LINK particles.

When a right-angle corner is formed in the chain of bonded LINK particles, the corner LINK particle decays into two SUBSTRATE particles, and the remaining LINK particles reconnect to each other (see Figure 2). This event fails to occur when there is no space to release the two SUBSTRATE particles. The LINK particles change into SUBSTRATE only in the above cases. Thus, the membrane never breaks up; it only changes size dynamically.

2.3 Geometrical Shapes of Membrane

In the original model, the LINK particles in the membrane are not allowed to move. However, in some models with the membrane system on lattice space, movement of the membrane is introduced [5, 11]. Here also, the bonded LINK particles move randomly, but there are some inhibition rules:

1. The angle of bonded LINK particles never becomes less than a right angle.
2. The bonded LINK particles don't cross each other.
3. Movement of bonded particles is constrained. The allowed local bond configurations are shown in Figure 2.

The first and the second rules have been inherited from the original model. They ensure that the membrane structure does not have an abnormal form that never uncoils. The third rule is required to avoid the disconnection of the LINK particles.

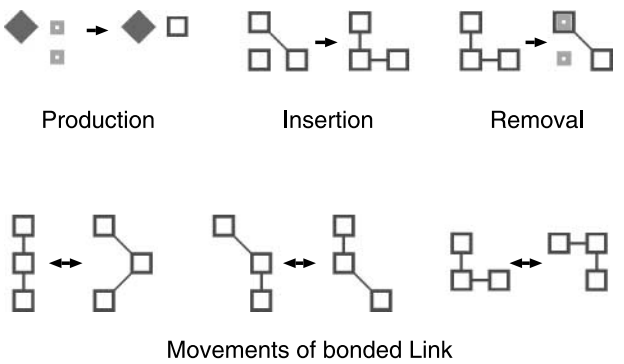

Figure 2. Metabolic rules (top), and local motions of the bonded LINKs (bottom). See the text for details.

3 Observations

3.1 Coherent Motion

When the membrane is expanded in one direction and withdrawn from the opposite side, the whole cell structure shifts to the expanding side. Whether the membrane is expanded or withdrawn is controlled by the metabolic process of the LINK particles and the CATALYST particle that generates them. On the other hand, the motion of the CATALYST particle is determined randomly, but it cannot cross the membrane. A coherent cell motion is achieved by the insertion and removal of the LINK particles on the membrane and the Brownian motion of the bonded LINK particles.

Cell behavior depends on some parameter values. In particular, the probability of removal of a LINK particle from a membrane is very influential. Figure 3 shows snapshots of cell dynamics for two different parameter values. The top four snapshots (A) are for high removal probability, and the bottom four (B) are for low removal probability. Table 1 shows other parameter values used in the simulation. We see that the membranes are relatively round in case A, and sharp in case B. This difference in cell shape will be discussed with respect to gradient-climbing behavior in the next subsection.

3.2 Climbing the Gradient

We study the cell motion when the environment has a gradient of SUBSTRATE particles. This should be one of the simplest environments in which the agent can perform sensory-motor coupling.

Figure 4 shows the trails of the cell movements when the cell starts from the center of the space. The gradient of the SUBSTRATE is controlled by the flow rates of the SUBSTRATE particles in the source and sink regions. In each time step, SUBSTRATE particles in the sink regions are moved to the source regions. By setting the size of the sink and source regions, we control the magnitude of the SUBSTRATE gradient. Here, the source is located at the top right at (15,15), and the sink at the bottom left at $(-15,-15)$. We use 3×3 squares for the sink and source regions. The particles in the sink region are transferred to the source region at a certain rate.

We then compare cases A and B. In case A, which has a high removal probability, a cell seems to approach the source region relatively straightforwardly. In contrast, a cell in case B, with a low removal probability, exhibits more exploratory and random motion relative to the source.

The trails of the movements are fluctuating. By summing different simulation runs, the gradient climbing motion is clearly depicted. Figure 5 shows the average distance from the source as a function of time for different values of the removal parameter. The space extends from -30 to 30 for each axis,

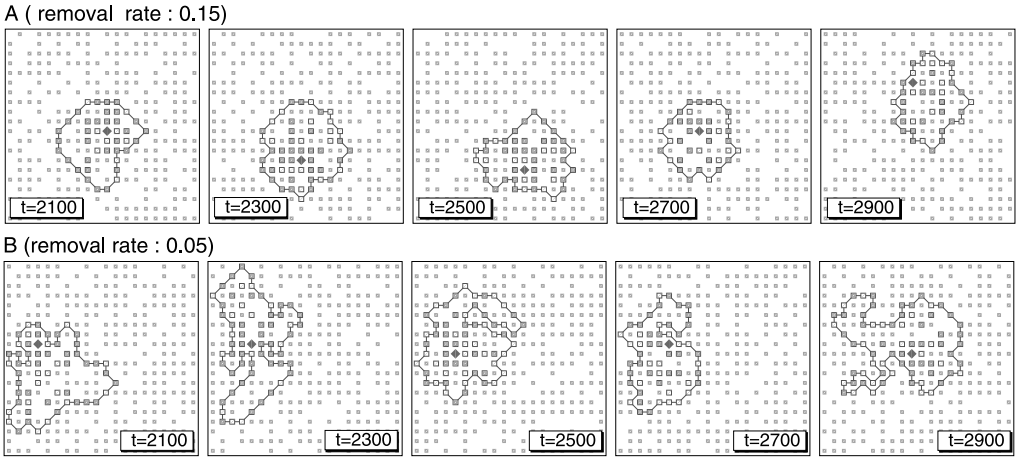

Figure 3. Snapshots of temporal cellular shapes under the two different parameter settings. With a higher removal rate (case A), the cellular shape becomes round. With a lower one (case B), the shape becomes sharp.

Table 1. The parameters used in our simulations.

Parameter	Value
Space size	60×60
Initial cell size	9×9
Initial SUBSTRATE density	0.7
Diffusion rate of the CATALYST	0.1
Diffusion rate of the LINK	0.4
Diffusion rate of the SUBSTRATE	0.4
Diffusion rate of the SUBSTRATE in the neighborhood of the LINK	0.2
Diffusion rate of the LINK in the neighborhood of the SUBSTRATE	0.2
Probability of production	1.0
Probability of insertion	0.1
Probability of movement of the membrane	0.5

and a cell starts at (0,0). The center of the source is placed at (18,0), and the center of the sink is placed at (−18,0). On increasing the removal rate, we notice that the cell approaches the source more swiftly.

This picture is verified by changing the magnitude of the gradient. Figure 6 shows the source approach rate of case A and case B with source and sink size changed from 0 to 7 × 7. When the size of the source increases, the SUBSTRATE gradient declines sharply. The approach rate is calculated by observing the frequency with which the cell is attracted to the source within 50,000 time steps over 100 simulation runs. The graph shows that the approach rates are larger in case A (large removal probability) than in case B (small removal probability). This result corresponds to Figure 4. The rate in case A (the upper line) increases when the source size grows. When there are more than 25 sites in the source, the increase seems to be saturated. On the other hand, in case B (the lower line), no climbing tendency is

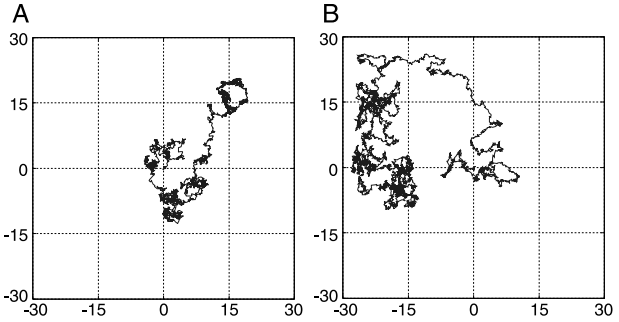

Figure 4. Spatial trails of cell movements with different random seeds are shown, where the SUBSTRATE particles flow from the top right corner (15,15) to the bottom left corner (−15,−15). The two plots correspond to cases A and B in Figure 3. In case A, cells are attracted to the top right corner, whereas in case B cells tend to explore without approaching it.

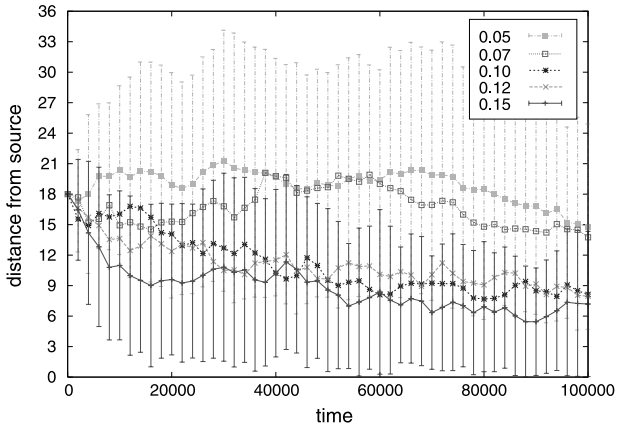

Figure 5. Average distances from the source of the SUBSTRATE are plotted for 30 different runs. They are compared for five different removal probabilities. In the event of high probability of removal, a cell tends to approach the source. Error bars are only shown when the removal parameters are 0.05 and 0.15, for visibility.

seen. When the source size increases, the approach rate decreases. This result indicates that the cell in the case with the larger removal probability has a sensitivity to the substrate gradient. Why a certain cell type shows a chemotactic tendency will become clear in the next section.

3.3 Biasing Metabolism

The modeled cells with a rounded shape exhibited gradient-climbing behavior, but those with a sharp shape did not. To reveal the mechanism for this outcome, we studied different combinations of reaction parameters and algorithms as follows:

(a) Case A (round shape) with the SUBSTRATE gradient

(b) Case A (round shape) without the SUBSTRATE gradient

(c) Case A (round shape) with the SUBSTRATE gradient, but no metabolism

(d) Case B (sharp shape) with the SUBSTRATE gradient

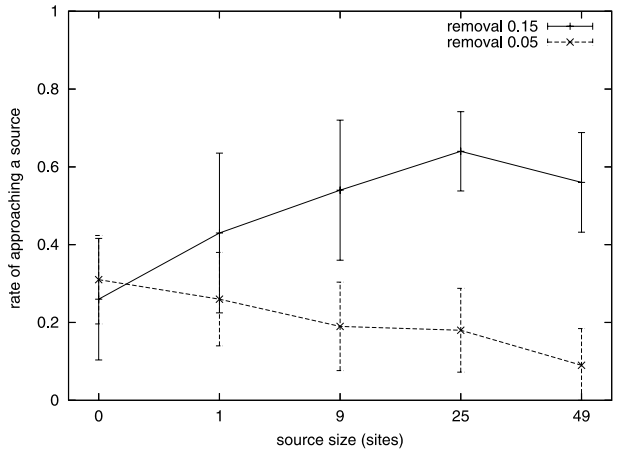

Figure 6. The difference between large and small removal parameters is made clearer by plotting the reaching probability against the SUBSTRATE source. Here the horizontal axis represents the size of the sink and source, which is proportional to the flow rate. Size 0 means there is no SUBSTRATE gradient. The vertical axis represents the probability of reaching the source during the initial 50,000 steps.

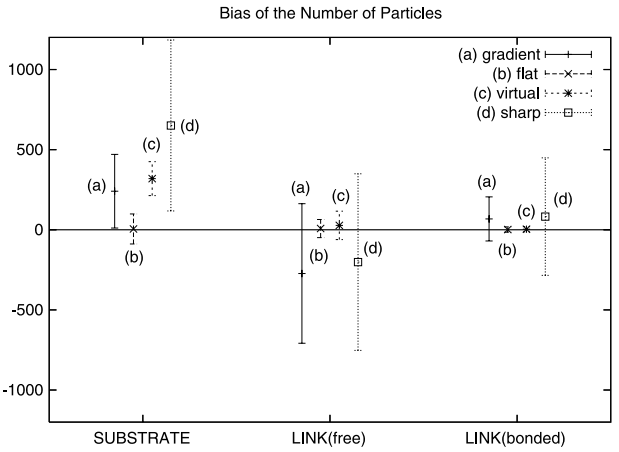

Figure 7. A biased distribution of the SUBSTRATE, the free LINK, and the bonded LINK particles exists within the cell. The values are calculated by subtracting the number of particles on the left side of the barycenter of the membrane from the number on the right side. We compare following four cases: (a) case A (removal = 0.15) with the SUBSTRATE gradient, (b) case A (removal = 0.15) without the SUBSTRATE gradient, (c) case A (removal = 0.15) with the SUBSTRATE gradient, but no metabolism, and (d) case B (removal = 0.05) with the SUBSTRATE gradient. What we see here is that cases (a) and (d) show significantly large fluctuations that are biased toward the opposite side from the source, in contrast with cases (b) and (c).

In case (c), the number of SUBSTRATE particles is conserved. No SUBSTRATE particle is consumed to make LINK particles or regenerated to remove them. This special setting is called a virtual SUBSTRATE. In the above case (a) alone, the cell exhibits positive chemotaxis; in the other three cases, positive chemotaxis disappears.

Figure 7 shows how the numbers of SUBSTRATE, free LINK, and bonded LINK particles fluctuate. It should be noted that the SUBSTRATE and the free LINK particles are counted within the cell. Each value is calculated by subtracting the number of the particles counted on the side to the left of the center of the membrane from the number to the right. In cases (a), (c), and (d), the SUBSTRATE particles are biased toward the side where the source is, because of the environmental gradient. However, the bias of the SUBSTRATE particles is smaller in case (a) than in case (c).

We found that the LINK particles accumulated in the cell on the side opposite the SUBSTRATE source in cases (a) and (d). In cases (b) and (c), the LINK particles are distributed equally on both sides of the cell. The reason for this biasing LINK particles in case (a) can be explained as follows. Due to the metabolic cycle, generation of one LINK particle consumes two SUBSTRATE particles, which can generate more space for new LINK particles.[1] Consequently, LINK particles are more abundant and SUBSTRATES are less abundant at the back. Without the metabolic cycle, as in the case (c), no new space is created when generating LINK particles. Therefore, abundance of LINK and SUBSTRATE particles are equally distributed around the CATALYST. This corresponds to the result that the insertion and removal events were more frequent on this side, as shown in Figure 8.

Conversely, the bonded LINK particles are biased to the source side in case (a). The increase of the cell size allows the CATALYST particle to move more freely, and this increases the chance they will come to the source side within the cell.

We compute the below value B to characterize the underlying events of this chemotactic behavior.

$$B = \sum_{i}^{n} \sigma_i, \qquad \sigma_i = \begin{cases} 1 & \text{for } x_i > \bar{x} \\ -1 & \text{for } x_i < \bar{x} \end{cases} \tag{2}$$

1 The LINK and SUBSTRATE particles are not mutually exclusive, but their diffusion rates to the neighboring vacant sites are put higher than to the already occupied sites. As a result, this condition sets a weak exclusion between the SUBSTRATE and LINK particles.

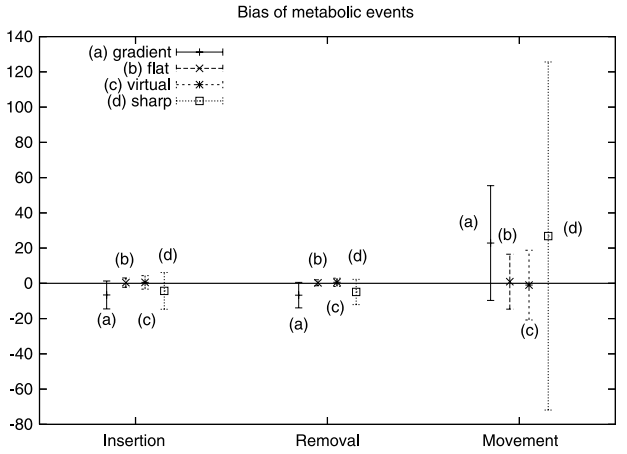

Figure 8. Average frequencies of the insertion, removal, and production of the LINK particle events occurring on the source side of the membrane with respect to the barycenter of a cell. We computed the number of events on the source side minus the number on the other side and plotted the difference on the vertical axis. We compare the four cases (a), (b), (c), and (d) as in Figure 7.

Here, x_i represents the x coordinate where the elementary events occur, $\overline{x}$ is the barycenter of the membrane particles, and n is the total number of target events. Figure 8 depicts the value B for each event. In case (a), which shows chemotaxis, the insertion, removal, and movements of the membrane events occur more frequently on the side further from the source of the SUBSTRATE particles. Different from the other three cases (b, c, d), the chemotactic behavior is caused by the bias of the metabolic processes. Case (c) (without the metabolic cycle of the SUBSTRATE to the LINK particles) does not exhibit the bias of events as in the flat condition (b). Comparing the chemotactic case (a) with the SUBSTRATE case (c), we see that the consumption and the provision of the SUBSTRATE particles may contribute to a directional bias of metabolic events caused by a biased distribution of the LINK particles.

We explain the mechanism of the gradient-climbing behavior in terms of these events as follows:

1. Free LINK particles aggregate on the internal side opposite to the source location. We call this the B (back) side.
2. Using the abundant LINK particles, the insertion and removal events of LINK particles become much more frequent on the B side.
3. A local movement of the membrane link is suppressed on the B side and enhanced on the other side, because the membrane on the B side is frequently regenerated.
4. This bias of the local movement leaves less space on the B side and much more space on the other side close to the source.
5. Since a CATALYST particle can move to the empty space, it stays longer on the source side. This tendency reinforces steps 1–4, and, on average, a cell shows chemotaxis.

A steeper gradient may induce this asymmetrical configuration of the membrane, so that with the increase in the source size, the cell approaches the source site more frequently, as seen in Figure 6.

In Figure 8d, we show on which part of the membrane the motile LINK particle was detected. In the sharp cell, the variance of this value is much larger than in the round cell. This means that the local movements of the bonded LINK particles fluctuate more in the sharp cell than in the round cell. The sharp cell has more pinning sites in the membrane, so that the cell does not always undergo the biased membrane movement. Thus, the sharp cell as a whole can't simply follow the outside gradient. We hypothesize that this pinning effect suppresses the chemotaxis in the case of the sharp cell.

4 Shape Transition Properties

We investigated the statistical properties of membrane shapes. To reveal how the shape changes, we computed a transition network among shapes in cases (a) [high removal probability (round shape)] and (b) [lower removal probability (sharp shape)] under the gradient of substrates. Then the networks are compared with those of case (c) [high removal probability without the gradient].

The algorithm for generating the shape transition network is the following: First we identify the shapes of the membrane with the longer life span (e.g., C or L or …); then we translate the time series of cell dynamics into a string of those membrane shapes (e.g., LCLCCRC). Second, the similarities among these strings are quantified by the Levenshtein distance (by counting how many insertions and deletions of characters are needed to match two character strings). Finally, similar shapes are clustered into the same groups when their similarities are higher than a given threshold. Then, the transition network of shapes in Figure 9 is obtained, where the nodes of the network are the clustered groups. The size of the nodes is proportional to the number of members in the group. Geometrically similar shapes are made to come close automatically in the network by connecting nodes with a spring

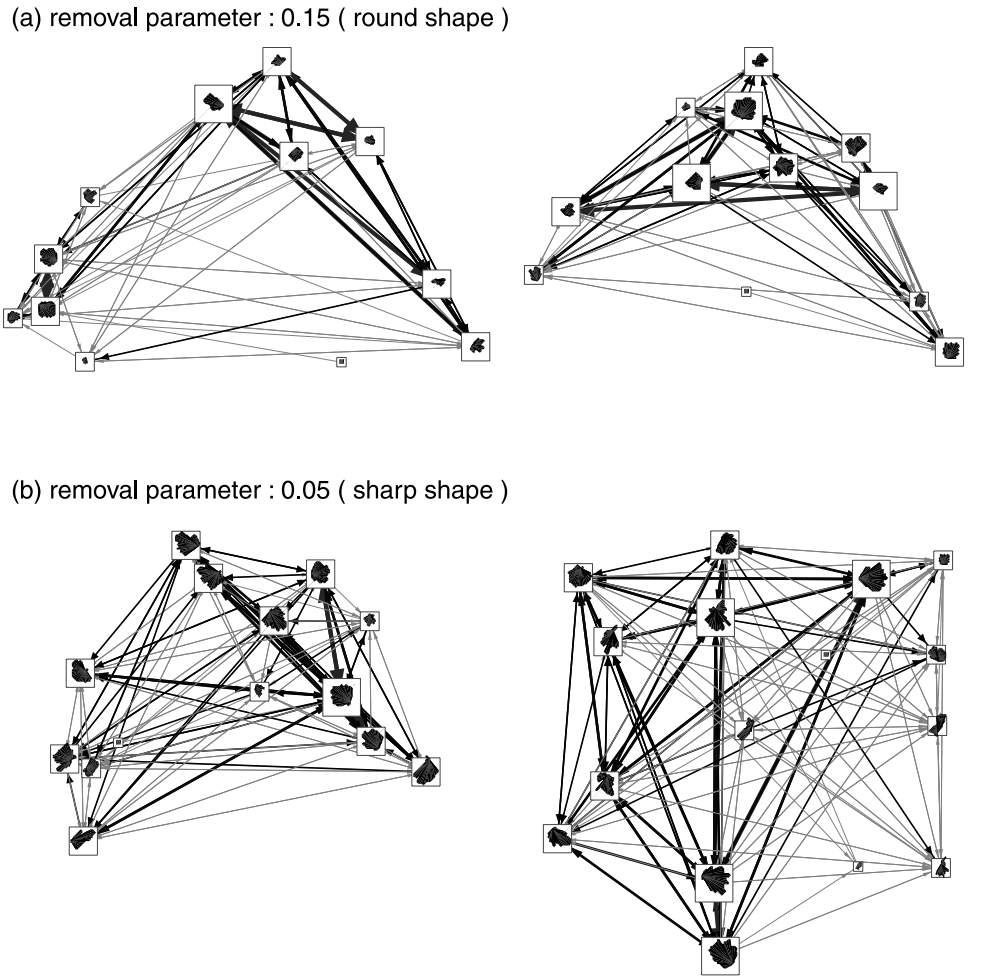

Figure 9. Examples of the shape transition networks in two different cases with gradient environments: (a) round shapes and (b) sharp shapes. The width of the lines reflects the number of connections. The nodes are roughly arranged according to the distances among them. These data are gathered during the 2,000 time steps with different random seeds.

whose coefficient is proportional to shape similarity. A node is connected to another node if the latter is the successor of the former in the simulation.

We see that the transition arms are localized among similar shapes in case (a), but in case (b), more different nodes appear than in case (a). The network topology is more linearly arranged and localized in case (a), but more uniformly distributed in case (b), except that we see some important nodes having many connections with other nodes. From this analysis, we see that case (b) allows many different membrane shapes but becomes less sensitive to the environmental gradient. On the other hand, case (a) has lower variety (or each shape has only a short life span), but shows chemotaxis. These observations imply that in real ameba-like cells, explorative and chemotactic phases can be objectively detected by the membrane shapes.

5 Discussion

In this article, we have demonstrated two things: First, membrane shape difference controls sensory-motor coupling, and in particular, chemotaxis. Second, self-movement emerges from a simple metabolic system with a self-generated boundary.

Regarding the first point, we demonstrated that a round cell climbed the gradient of the SUBSTRATE, but a sharp cell could not. But we also noticed that a round cell showed a large fluctuation of motion and chemotaxis appeared as a disposition of the cell. This is because a cell has no sensory organs on the membrane, but by creating an asymmetrical internal fluctuation of particles, it behaves as if it could perceive the environment. In this sense, the geometry of a membrane shape controls sensitivity to the environment. This geometry-induced fluctuation is the source of fluctuation of motion, which we think is tightly linked with the idea of biological autonomy.

There is empirical evidence to support the above conclusions. It has been found that by pushing the cytoplasm of a cell, one can elicit directional locomotion [20]. The asymmetrical change of a boundary shape causes polarization of actin and myosin fragments, and their interaction causes a straightforward motion. This internal polarization of chemicals is similar to our observation. In both their case and our modeling, a kind of internal bias is necessary for breaking symmetry to cause self-movement.

We have put forward a novel view of chemotaxis. If we take chemotaxis as an automatic entrainment between the internal state of a cell and the external chemical gradient, we can't claim it is based on biological autonomy. That is, if a cell always climbs up the gradient, the cell's behavior is uniquely determined by the environmental condition, and we see no autonomy here. In order to ground the self-movement as a property of a life system, we should consider variations and fluctuations of the behavioral pattern associated with the self-movement. By identifying different behaviors in the same conditions, or the same behaviors in different conditions, we can distinguish self-movement from externally driven (i.e., passive) motion. Therefore, we expect a valid simulation of autonomous chemotaxis to show how a pattern of chemotaxis fluctuates and how a rigid sensory-motor coupling relaxes. We thus study the nature of chemotaxis by controlling the balance between the internal dynamics and the membrane shape.

As for the second point, we demonstrated an abstract cell system that is both self-maintained and capable of self-movement. In previous work [14], we demonstrated that an autopoietic cell could move by continuously self-repairing the membrane, but failed to show any gradient-climbing behavior. This may be due to the fact that the autopoietic cell can only survive in a narrow range of the environmental SUBSTRATE density. Compared with that autopoietic cell model, in this study we used a more stable cell that never loses its membrane. Thus, the new cell can survive in a wider range of SUBSTRATE densities, but not in all environments. A cell membrane shrinks into the minimal loop and stack.

In view of the importance of a stable membrane, we contend that a kind of homeostasis is a basis for self-movement. Homeostasis is due to a self-regulating system that sustains a membrane by internal chemical processes. Homeostasis isn't simply preserving cell identity; it also promotes self-movement with minimal cognitive behaviors. We argued in [6] that the transition from homeostatic self (self maintained statically) to homeodynamic self (self dynamically sustained) emphasizes the potentiality of homeostasis.

A self-moving oil droplet is an empirical example of a homeodynamic system [15, 3]. An oil droplet mainly made of an acid precursor shows autonomous, sustained movement through the aqueous medium. Movement is induced through symmetry breaking and is sustained by a self-generated pH gradient inside the droplet that triggers a Marangoni instability and convection in the oil phase. As the result, the oil droplet shows a directional movement and appears to sense the pH gradient.

There have been studies using chemical systems to manipulate a robot or agent, instead of using neural networks [4, 9]. Diffusion-based couplings mediating sensor and motor devices are evolved in these works. The ability to study the sensor and motor devices with a simple chemical system is a big advantage of this model. We do not need special devices for sensor and motor functions. Instead, the dynamics of the membrane work as the sensor and motor. In addition, because our model uses simple components and rules, our model can be implemented by simple homogeneous module robots, moving and connecting with each other. This will be a promising application of the SCL model in the field of distributed robotics (e.g. module robots displaying amoebic locomotion [7]).

To conclude, we have demonstrated at least a possible link between internal chemistry and membrane shape that sustains an adequate cell boundary, causing a whole cell to move randomly but also purposefully (chemotaxis). Our next challenge is to study the necessary condition for bootstrapping complex sensory-motor coupling from a simple homeodynamic system.

Acknowledgments

This work is partially supported by the 21st Century COE (Center of Excellence) program (Research Center for Integrated Science) of the Ministry of Education, Culture, Sports, Science, and Technology, Japan, and the ECAgent project, sponsored by the Future and Emerging Technologies program of the European Community (IST-1940).

References

1. Bentley, K., & Clack, C. (2004). The artificial cytoskeleton for lifetime adaptation of morphology. In J. Pollack, M. Bedau, P. Husbands, T. Ikegami, & R. A. Watson (Eds.), *Workshop proceedings of the 9th International Conference on the Simulation and Synthesis of Living Systems* (pp. 13–16).

2. Bottino, D., Mogilner, A., Roberts, T., Stewart, M., & Oster, G. (2002). How nematode sperm crawl. *Journal of Cell Science*, *115*(2), 367–384.

3. Hanczyc, M. M., Toyota, T., Ikegami, T., Packard, N., & Sugawara, T. (2006). Chemistry at the oil-water interface: Self-propelled oil droplets. *Journal of the American Chemical Society*, *129*(30), 9386–9391.

4. Husbands, P., Smith, T., Jakobi, N., & O'Shea, M. (1998). Better living through chemistry: Evolving gasnets for robot control. *Connection Science*, *10*(3–4), 185–210.

5. Hutton, T. J. (2004). A functional self-reproducing cell in a two-dimensional artificial chemistry. In J. Pollack, M. Bedau, P. Husbands, T. Ikegami, & R. A. Watson (Eds.), *Artificial life IX: Proceedings of the 9th International Conference on the Simulation and Synthesis of Living Systems* (pp. 444–449). Cambridge, MA: MIT Press.

6. Ikegami, T., & Suzuki, K. (2007). From homeostatic to homeodynamic self. *BioSystems*, *91*(2), 388–400.

7. Ishiguro, A., Shimizu, M., & Kawakatsu, T. (2006). A modular robot that exhibits amoebic locomotion. *Robotics and Autonomous Systems*, *54*(8), 641–650.

8. Karakozova, M., Kozak, M., Wong, C. C., Bailey, A. O., Yates, J. R., Mogilner, A., Zebroski, H., & Kashina, A. (2006). Arginylation of beta-actin regulates actin cytoskeleton and cell motility. *Science*, *313*(5784), 192–196.

9. McHale, G., & Husbands, P. (2004). Quadrupedal locomotion: Gasnets, ctrnns and hybrid ctrnn/pnns compared. In J. Pollack, M. Bedau, P. Husbands, T. Ikegami, & R. A. Watson (Eds.), *Artificial life IX: Proceedings of the 9th International Conference on the Simulation and Synthesis of Living Systems* (pp. 106–113). Cambridge, MA: MIT Press.

10. McMullin, B., & Varela, F. R. (1997). Rediscovering computational autopoieses. In P. Husband & I. Harvey (Eds.), *Proceedings of the 4th European Conference on Artificial Life* (pp. 38–47). Cambridge, MA: MIT Press.

11. McMullin, B., & Groß, D. (2001). Towards the implementation of evolving autopoietic artificial agents. In J. Kelemen & P. Sosik (Eds.), *6th European Conference on Artificial Life* (pp. 440–443).

12. Nishimura, S. I., & Sasai, M. (2004). Inertia of chemotactic motion as an emergent property in a model of an eukaryotic cell. In J. Pollack, M. Bedau, P. Husbands, T. Ikegami, & R. A. Watson (Eds.), *Artificial life IX: Proceedings of the 9th International Conference on the Simulation and Synthesis of Living Systems* (pp. 410–414). Cambridge, MA: MIT Press.

13. Parent, C. A., & Devreotes, P. N. (1999). A cell's sense of direction. *Science*, *284*(5415), 765–770.

14. Suzuki, K., & Ikegami, T. (2004). Self-repairing and mobility of simple cell model. In J. Pollack, M. Bedau, P. Husbands, T. Ikegami, & R. A. Watson (Eds.), *Artificial life IX: Proceedings of the 9th International Conference on the Simulation and Synthesis of Living Systems* (pp. 421–426). Cambridge, MA: MIT Press.

15. Toyota, T., Tsuha, H., Yamada, K., Takakura, K., Ikegami, T., & Sugawara, T. (2006). Listeria-like motion of oil droplets. *Chemistry Letters*, *35*, 708–709.

16. Uchida, K. S., Kitanishi-Yumura, T., & Yumura, S. (2003). Myosin ii contributes to the posterior contraction and the anterior extension during the retraction phase in migrating dictyostelium cells. *Journal of Cell Science*, *116*(Pt. 1), 51–60.

17. Van Haastert, P. J., & Devreotes, P. N. (2004). Chemotaxis: Signalling the way forward. *National Review of Molecular and Cell Biology*, *5*(8), 626–634.

18. Varela, F. R. (1979). *Principles of biological autonomy*. New York: North Holland.

19. Varela, F. R., Maturana, H. R., & Uribe, R. (1974). Autopoiesis: The organization of living systems, its characterization and a model. *BioSystems*, *5*, 187.

20. Verkhovsky, A. B., Svitkina, T. M., & Borisky, G. G. (1999). Self-polarization and directional motility of cytoplasm. *Currrent Biology*, *9*, 11–20.

21. Yumura, S., & Fukui, Y. (1998). Spatiotemporal dynamics of actin concentration during cytokinesis and locomotion in dictyostelium. *Journal of Cell Science*, *111*(15), 2097–2108.

22. Yumura, S., Mori, H., & Fukui, Y. (1984). Localization of actin and myosin for the study of ameboid movement in dictyostelium using improved immunofluorescence. *Journal of Cell Biology*, *99*(3), 894–899.

23. Iijima, M., & Devreotes, P. (2007). Temporal and spatial regulation of chemotaxis. *Developmental Cell*, *3*(4), 469–478.